Bioorg. Med. Chem. Lett. 41 (2021) 127992

Contents lists available at ScienceDirect

Bioorganic & Medicinal Chemistry Letters

journal homepage: www.elsevier.com/locate/bmcl

Discovery of *N*-amido-phenylsulfonamide derivatives as novel microsomal prostaglandin E_2 synthase-1 (mPGES-1) inhibitors

Misong Kim [a,1], Geuntae Kim [a,1], Minji Kang [a], Dohyeong Ko [a], Yunchan Nam [a], Chang Sang Moon [a], Heung Mo Kang [a], Ji-Sun Shin [b], Oliver Werz [c], Kyung-Tae Lee [b,*], Jae Yeol Lee [a,d,*]

[a] Research Institute for Basic Sciences and Department of Chemistry, College of Sciences, Kyung Hee University, Seoul 02447, Republic of Korea
[b] Department of Life and Nanopharmaceutical Science, College of Pharmacy, Kyung Hee University, Seoul 02447, Republic of Korea
[c] Department of Pharmaceutical/Medicinal Chemistry, Institute of Pharmacy, Friedrich-Schiller-University Jena, Philosophenweg 14, 07743 Jena, Germany
[d] KHU-KIST Department of Converging Science and Technology, Kyung Hee University, Seoul 02447, Republic of Korea

ARTICLE INFO

Keywords:
Inflammation
PGE_2
Bioisosteric replacement
Molecular docking
mPGES-1 inhibitor

ABSTRACT

Our previous research showed that *N*-carboxy-phenylsulfonyl hydrazide (scaffold A) could reduce LPS-stimulated PGE_2 levels in RAW 264.7 macrophage cells by an inhibition of mPGES-1 enzyme. However, a number of scaffold A derivatives showed the drawbacks such as the formation of regioisomers and poor liver metabolic stability. In order to overcome these synthetic and metabolic problems, therefore, we decided to replace *N*-carboxy-phenylsulfonyl hydrazide (scaffold A) with *N*-carboxy-phenylsulfonamide (scaffold B) or *N*-amido-phenylsulfonamide frameworks (scaffold C) as a bioisosteric replacement. Among them, **MPO-0186** (scaffold C) inhibited the production of PGE_2 (IC_{50}: 0.24 μM) in A549 cells via inhibition of mPGES-1 (IC_{50}: 0.49 μM in a cell-free assay) and was found to be approximately 9- and 8-fold more potent than **MK-886** as a reference inhibitor, respectively. A molecular docking study theoretically suggests that **MPO-0186** could inhibit PGE_2 production by blocking the PGH_2 binding site of mPGES-1 enzyme. Furthermore, **MPO-0186** demonstrated good liver metabolic stability and no significant inhibition observed in clinically relevant CYP isoforms except CYP2C19. This result provides a potential starting point for the development of selective and potent mPGES-1 inhibitor with a novel scaffold.

Prostaglandin E_2 (PGE_2) is a widely distributed prostaglandin in the human body and the principal prostaglandin of acute inflammation and of chronic diseases such as rheumatoid arthritis and inflammatory bowel disease.[1–2] Therefore, the interference of PGE_2 production may alleviate inflammatory symptoms such as fever, arthritis, and inflammatory pain.[2] The biosynthetic pathway of PGE_2 involves three sequential enzymatic actions from arachidonic acid (AA): AA is released from the membrane by phospholipase A_2 (PLA_2) and then converted to PGH_2 by cyclooxygenase 1 and 2 (COX-1 and COX-2), followed by the subsequent isomerization of PGH_2 into PGE_2 by the terminal enzymes, prostaglandin E synthases (three isoforms: cPGES, mPGES-1 and mPGES-2).[3–5]

The successful modulation of PGE_2 via the inhibition of one of three sequential enzymatic actions may prevent or retard the inflammatory symptoms. In order to avoid the gastrointestinal (GI) side effects of nonsteroidal anti-inflammatory drugs (NSAIDs) inhibiting two isoforms of COX, selective COX-2 inhibitors (coxibs) such as celecoxib and rofecoxib with lower risk of GI injury were developed.[6] However, these selective coxibs were revealed to increase the risk for cardiovascular events due to the prevention of prostaglandin productions [in particular, prostacyclin (PGI_2)] of downstream of PGH_2 as well as PGE_2.[7] Thus, valdecoxib (Bextra®) and rofecoxib (Vioxx®) were withdrawn from the market in 2004 and 2005, respectively.[8] Meanwhile, microsomal prostaglandin E_2 synthase-1 (mPGES-1) stimulated by inflammatory stimuli catalyzes the terminal step in the biosynthesis of COX-2-derived PGE_2 from PGH_2.[9] Thus, the selective inhibition of mPGES-1 is a safe therapeutic concept without any GI side effects compared to traditional NSAIDs and coxibs. Therefore, various mPGES-1 inhibitors have been reported in the literatures (Fig. 1).[10] Unfortunately, drug development

* Corresponding authors at: Research Institute for Basic Sciences and Department of Chemistry, College of Sciences, Kyung Hee University, Seoul 02447, Republic of Korea (J.Y. Lee).
E-mail addresses: ktlee@khu.ac.kr (K.-T. Lee), ljy@khu.ac.kr (J.Y. Lee).
[1] The contribution of the authors is equal.

https://doi.org/10.1016/j.bmcl.2021.127992
Received 2 January 2021; Received in revised form 11 March 2021; Accepted 19 March 2021
Available online 26 March 2021

has been halted due to lack of potent inhibitors and a specific drug-induced liver injury (DILI) of LY3023703.[11] Only a few mPGES-1 inhibitors including GRC 27,864 have entered clinical trials.[12–13] Therefore, there is still an unmet need for the development of more potent and safer mPGES-1 inhibitors.

We had recently identified selective mPGES-1 inhibitors containing *N*-carboxy-phenylsulfonyl hydrazide scaffold (scaffold A) for the development of anti-inflammatory drugs (Fig. 2).[14–17] Despite the good inhibitory activities against PGE_2 production and mPGES-1 enzyme (for example, **MPO-0063** in Table 1), major drawbacks of phenylsulfonyl hydrazide derivatives were the inevitable formation of two regioisomers depending on the reaction position (that is, two nitrogen atoms in phenylsulfonyl hydrazide scaffold) [15] and poor pharmacokinetic properties such as liver microsomal stability and plasma stability (data of **MPO-0063** in Table 2). On the other hand, bioisosterism represents one approach used by the medicinal chemist for the rational modification of lead compounds into safer and more clinically effective agents via replacement of functional groups or scaffolds.[18] In order to overcome these problems associated to phenylsulfonyl hydrazide scaffold, we decided to investigate the effect of replacing *N*-carboxy-phenylsulfonyl hydrazide (scaffold A) with *N*-carboxy-phenylsulfonamide (scaffold B) and *N*-amido-phenylsulfonamide frameworks (scaffold C), respectively, as shown in Fig. 2.

In the present study, we examined the effects of synthetic compounds featuring three unique scaffolds on PGE_2 production, mPGES-1 activity, CYP450 activity, liver microsomal stability, and plasma stability, respectively (Fig. 2). In addition, a flexible molecular docking was also carried out using the Molegro Virtual Docker (MVD) software package for the comparison of binding modes of three unique scaffolds.

The representative synthesis of *N*-carboxy-phenylsulfonyl hydrazide **11**, *N*-carboxy-phenylsulfonamide **12** and *N*-amido-phenylsulfonamide frameworks **13** has been accomplished in three steps of reaction according to our previously reported procedure as illustrated in Scheme 1.[14–16] Phenylsulfonyl hydrazide **3a-b** and phenylsulfonamide **8** were prepared from the reaction of phenylsulfonyl chloride **1** with phenylhydrazine **2** and benzylamine **7**, respectively, in presence of triethylamine (TEA) or diisopropylethylamine (DIPEA: Hünig's base). Phenyl chloroformate **6** was prepared in quantitative yield from the reaction of phenol **4** with 0.5 equiv of triphosgene **5** in presence of Hünig's base. The coupling reaction of chloroformate **6** with phenylsulfonyl hydrazide **3** or phenylsulfonamide **8** afforded the desired *N*-carboxy-phenylsulfonyl hydrazide **11a-b** (previously reported kinetic product) [15] and *N*-carboxy-phenylsulfonamide **12**, respectively, in 73–90% yield. In the case of *N*-amido-phenylsulfonamide derivatives **13a-b**, phenylsulfonamide **8** was treated with 0.5 equiv of triphosgene **5** to afford *N*-chlorocarbonyl phenylsulfonamide **9,** which was finally coupled with 4-substituted aniline **10** in the presence DIPEA and 4-(dimethylamino) pyridine (DMAP) as a catalyst to afford the desired *N*-amido-phenylsulfonamide derivatives **13a-b**.

The synthesized compounds were evaluated using EIA kit (Enzo Life Sciences, Inc., Farmingdale, NY, USA) for their inhibitory activity against PGE_2 production in A549 human lung cancer cell lines.[19] In order to check that the suppressive effects of synthesized compounds on PGE_2 production could be attributable to non-specific cytotoxicity, we examined the cytotoxic effect of synthesized compounds in A549 cells in the presence of interleukin-1β (1 ng/mL) using MTT assays.[20] None of the compounds affected the viabilities of A549 cells at 1 μM concentration over 24 h. Therefore, all compounds were screened for their abilities to suppress PGE_2 production in IL-1 β (1 ng/mL)-stimulated A549 cells over 24 h.[21] **PF-4693627** (@ 1 μM) was used as a reference inhibitor [22] and suppressed the PGE_2 synthesis (IC_{50} = 0.52 μM under our assay condition) as expected (Table 1 and Fig. 3). Their exact IC_{50} values were obtained through three independent experiments and summarized into Table 1. All synthesized compounds displayed good inhibitory activities against PGE_2 production (IC_{50} = 0.15 to 0.61 μM) in the order of scaffold A ~ scaffold B > scaffold C. Compound **11b** (**MPO-0144**: scaffold A) was found to be the most potent inhibitor against PGE_2 production (IC_{50} value of 0.15 μM). In the meanwhile, it was previously reported that **11a** (**MPO-0063**) and **12** (**MPO-0112**) also inhibited LPS-induced PGE_2 production with IC_{50} = 0.06 and 0.34 μM, respectively, in RAW 264.7 macrophages.[15,23]

To further confirm whether compounds could act on human mPGES-1, we carefully assessed their inhibitory activities against human cell-free mPGES-1 using microsomes of IL-1β-stimulated A549 cells. **PF-4693627** and **MK-886** were used as reference inhibitors and the potency of **PF-4693627** (IC_{50} = 3 nM) was almost consistent with the reported value (Fig. 4A).[22] Compound **11a** (**MPO-0063**: scaffold A) carrying a phenylsulfonyl hydrazide group showed an IC_{50} value of 0.61 μM. However, compound **11b** (**MPO-0144**: scaffold A) with 3-chloro substituent within *N*-phenyl ring completely failed to inhibit mPGES-1 up to 30 μM. Compound **12** (**MPO-0112**: scaffold B), *N*-carboxy-phenylsulfonamide and a methylene analog of **11a,** exhibited some reduced activity with an IC_{50} value of 7.37 μM compared to that of **11a**. Compound **13a** (**MPO-0180**: scaffold C), *N*-amido analog of **12** (**MPO-0112**: scaffold B), displayed strong loss of potency (IC_{50} = >30 μM). On the other hand, *N*-carboxy-phenylsulfonamide (or *N*-phenylcarbamate) scaffold B of **12** (**MPO-0112**) exhibited poor liver microsomal stability of all tested species and intermediate inhibition of hERG channel (Table 2). So, we decided not to proceed the further investigation of substituent effects on **12** (**MPO-0112**) activity. As shown in Fig. 1, the

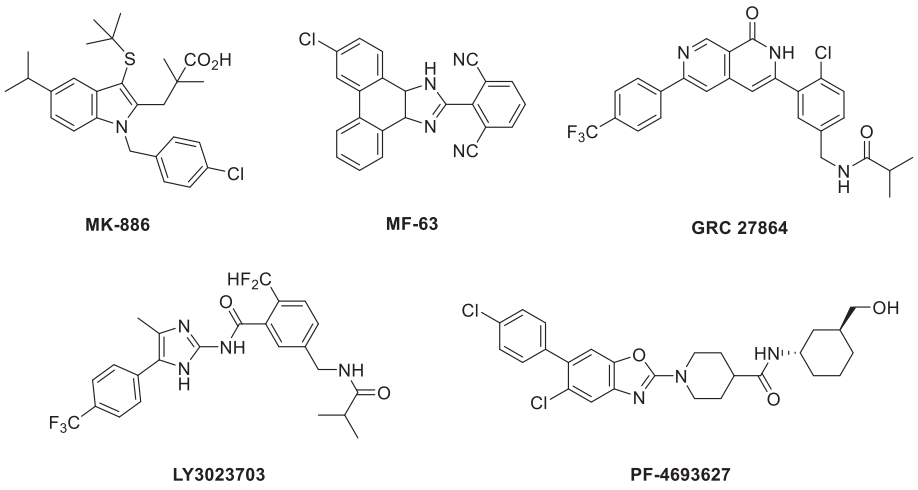

Fig. 1. Previously reported mPGES-1 inhibitors.

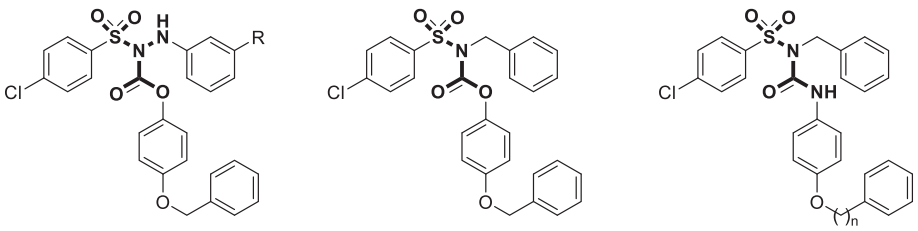

Fig. 2. Structural modification of mPGE1-1 inhibitors based on their biological activities and *in vitro* pharmacokinetic parameters.

Table 1
Biological data and MolDock Scores of *N*-carboxy-phenylsulfonyl hydrazide, *N*-carboxy-phenylsulfonamide, and *N*-amido-phenylsulfonamide derivatives.

Entry (Lab. ID)	Scaffold	Cell viability (μM) [a]	PGE_2 IC_{50} (μM) [b, c]	mPGES-1 IC_{50} (μM) [b, d]	MolDock Score [e]
11a (MPO-0063)	scaffold A	> 1	0.19 ± 0.05	0.61[f]	−142.6
11b (MPO-0144)	scaffold A	> 1	0.15 ± 0.02	>30	−135.4
12 (MPO-0112)	scaffold B	> 1	0.16 ± 0.01	7.37 [g]	−147.2
13a (MPO-0180)	scaffold C	>1	0.61 ± 0.04	>30	−136.9
13b (MPO-0186)	scaffold C	>1	0.24 ± 0.05	0.49	−158.7
PF-4693637 [h]		>1	0.52 ± 0.04 [i]	0.003 [j]	−133.8
MK-886 [h]		>1 [g]	2.10 [k]	3.90 [g]	−143.4

[a]Cytotoxicity of each compound using MTT assay; [b] Data are presented as the means ± SDs of three independent experiments; [c] The inhibition value of IL-1β (1 ng/mL)-stimulated PGE_2 production in A549 cells; [d] The mPGES-1 activity was evaluated under cell-free conditions by measuring PGE_2 production; [e] MolDock score during docking in the active site of mPGES-1 (PDB code: 4AL0) by using MVD 2012.5.5.0.; [f] Our previously reported data [14]; [g] Our previously reported data [23]; [h] Reference inhibitors [22]; [i] 16% inhibition at 1 μM under our assay condition (Figure 3); [j] This data is in agreement with the literature (IC_{50} = 3.0 nM)[22]; [k] The data of literature[24].

Table 2
Preliminary ADME data of three scaffold compounds.

	11a (MPO-0063)	**12 (MPO-0112)**	**13b (MPO-0186)**
PGI_2 (IC_{50}) [a]	0.25 μM	2.0 μM	1.0 μM
hERG (IC_{50})	9.60 μM	5.2 μM	>10 μM
CYP450 activity (% of control activity at 10 μM)			
CYP1A2	75.7	99.4	69.4
CYP2C9	88.4	97.0	99.9
CYP2C19	77.9	56.9	8.7
CYP2D6	57.1	>100	98.8
CYP3A4	73.6	>100	92.5
Liver microsomal stability (%remaining during 30 min at 1 μM)			
human	66.6	44.9	>100
dog	48.5	37.7	86.4
rat	16.3	44.1	74.5
mouse	42.2	53.4	79.0
Plasma Stability (%remaining during 30 min at 10 μM)			
human	<1	>100	45.0
rat	<1	2.1	1.3

[a] Inhibitory effect on IL-1 β (1 ng/mL)-stimulated PGI_2 production in A549 human lung cancer cell lines.

recently reported three mPGES-1 inhibitors have a linear or U-shaped conformation compared to the compact conformation of **MK-886** and **MF-63**. Therefore, the introduction of additional three methylene units in benzyloxyphenyl moiety of **13a**, resulting in compound **13b** (**MPO-0186**: scaffold C), improved the activity (IC_{50} = 0.49 μM) as shown in Fig. 4B. This compound **13b** (**MPO-0186**) represents the most potent mPGES-1 inhibitor within this study, which is 8-fold more active than **MK-886** as a competitive inhibitor (Table S1 of Supplementary data).

Molecular docking studies were performed to investigate and get a better understanding of the observed SAR among these three scaffolds by using the recently reported X-ray crystallized structure of mPGES-1 (PDB code: 4AL0). The docking studies were performed using Molegro Virtual Docker (MVD) 2012.5.5.0 for Windows. First of all, we identified one cavity with a volume 51 $Å^3$ located in close proximity to GSH (glutathione) as a cofactor by the same software, which can automatically detect cavities from protein surfaces. The putative active site of the enzyme was defined to include residues within a 15 Å radius to this cavity. The docking wizard of MVD 2012.5.5.0 was used to dock all compounds together with **PF-4693637** and **MK-886** as mPGES-1 inhibitors for comparison. During the docking process, the top pose was deposited for each ligand based on the MolDock score, which was inserted in Table 1. The appropriate correlation between IC_{50} values and MolDock Scores of synthesized compounds was found except **PF-4693637**. Interestingly, **PF-4693637** with the best potency (IC_{50} = 3 nM) displayed the lowest MolDock Score (-133.8), which would mean that this compound might bind to an enzyme at a site other than the active site including GSH and thus play a role as an allosteric inhibitor, even though that any X-ray crystal structure of **PF-4693637** and mPGES-1 complex has not been reported until now. In order to confirm this hypothesis, the further docking study was carried out using the recently reported X-ray crystal structures and afforded the very similar results, regardless of whether or not GSH is present in active site of mPGES-1 (Table S1 in Supplementary data). **11b** (**MPO-0144**) and **13a** (**MPO-0180**) displayed lower MolDock Score (-135.4 and −136.9, respectively), which was consistent with their weak potencies against mPGES-1. When the oxygen of **12** (**MPO-0112**: scaffold B) was replaced with NH in **13a** (**MPO-0180**: scaffold C), the hydrogen bond energy was increased but the total interaction energy was decreased regardless of whether or not GSH is present in active site of mPGES-1 (Table S2, Fig. S1, Fig. S2, and Supplementary data). Thus, **12** (**MPO-0112**: scaffold B) showed higher MolDock score (-147.2) and better inhibitory activity on mPGES-1 than **13a** (**MPO-0180**: scaffold C). On the other hand, the most active **13b** (**MPO-018b)** showed the highest MolDock score (-158.7), which supports that this compound could inhibit PGE_2 production by blocking the active site of enzyme. In order to explain the difference in the activity against mPGES-1 between **13a** (**MPO-0180**; IC_{50} = >30 μM) and **13b** (**MPO-0186**; IC_{50} = 0.49 μM) according to the length of methylene unit, the highest-ranking docking pose of each compound was analyzed to further investigate the interaction of the docked conformation within the active site. Before the analysis, Asp49,

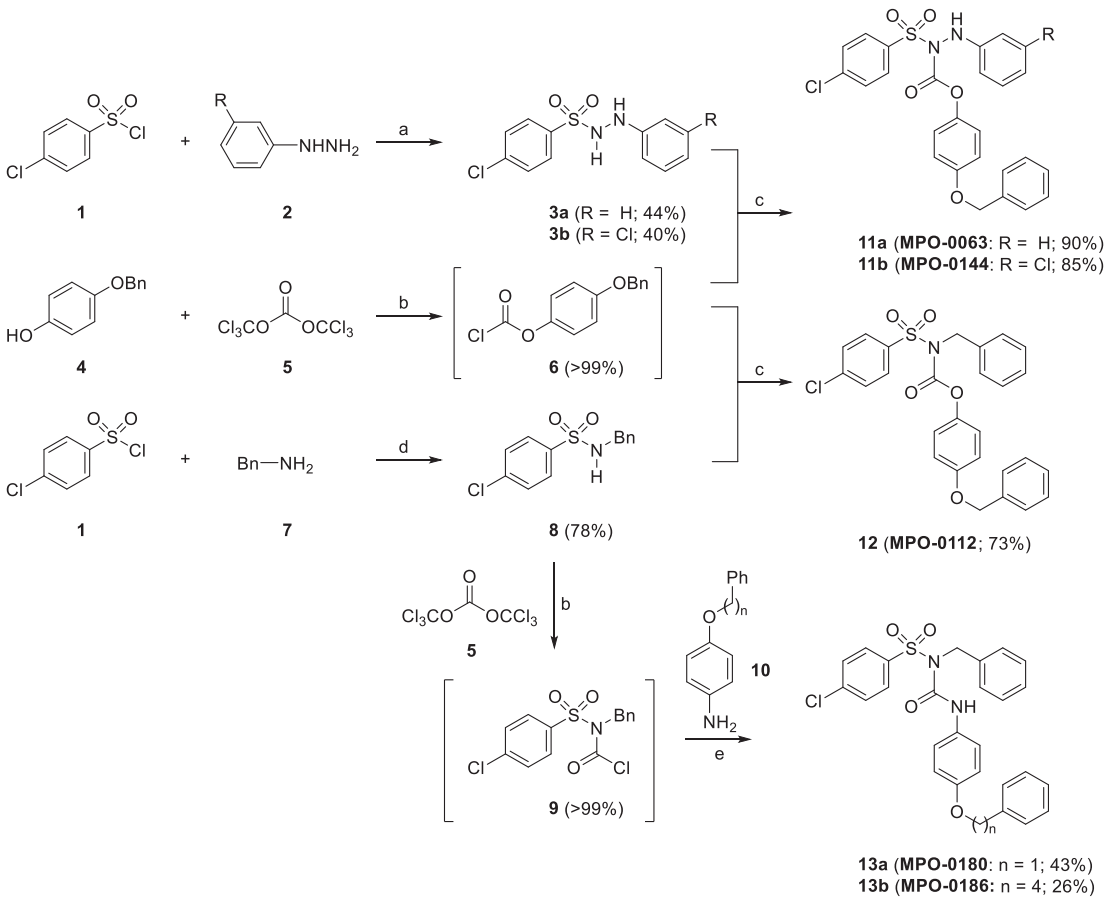

Scheme 1. Reagents and conditions: (a) TEA, dry THF, 0 ℃ to rt, 3 h; (b) DIPEA, dry THF, 0 ℃, 2–4 h; (c) TEA, dry THF, rt, 2–4 h; (d) DIPEA, dry THF, rt, 2 h; (e) DIPEA, DMAP (*cat.*), dry THF, rt, 12 h.

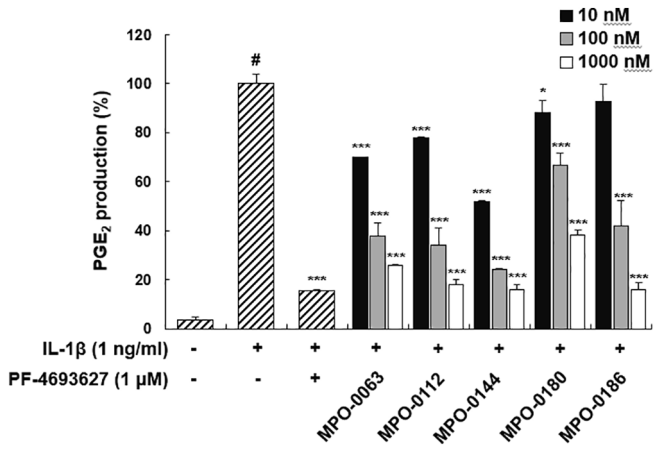

Fig. 3. Effect of synthesized compounds on IL-1 β (1 ng/mL)-stimulated PGE_2 production in A549 human lung cancer cell lines. Cells were treated with only IL-1 β (1 ng/ml) or along with the compounds (10, 100, or 1000 nM) for 24 h. Levels of PGE_2 in culture media were quantified using EIA kit. **PF-4693627** (1 μM) was used as a reference inhibitor. $^{\#}p < 0.05$ versus the control group; $^{***}p < 0.001$ versus the IL-1 β -stimulated group; significant differences between groups were determined using ANOVA and Dunnett's post-hoc test.

Asp126 and Ser127 were found to be key residues which are reported in the literature.[25] Fig. 5a-d represent the docking poses of **13a** (**MPO-0180**) and **13b** (**MPO-0186**), respectively. In the case of **13a** (**MPO-0180**), one oxygen atom of the sulfone moiety constituted two hydrogen bond interactions with glutathione (3.19 Å) and Arg126 (2.97 Å), and one nitrogen atom of the urea moiety also established a hydrogen bond interaction with glutathione (3.35 Å) as shown in Fig. 5a-b. The sum of hydrogen bond energy was found to be −6.7 value. The other major interaction was hydrophobic interactions between the ligand and neighboring amino acids as shown in Fig. 5b. With respect to **13b** (**MPO-0186**), there were also major interactions between this ligand and amino acids of the active site (Fig. 5c-d). One oxygen atom of the sulfone moiety constituted two short and strong hydrogen bond interactions with glutathione (2.96 Å) and Ser127 (2.74 Å). One nitrogen atom of the urea moiety exhibited an additional hydrogen bond interaction with glutathione (2.92 Å) as shown in Fig. 5c-d. The sum of hydrogen bond energy was found to be −7.5 value. The other major interaction was hydrophobic interactions between the ligand and neighboring amino acids as shown in Fig. 5d. The total interaction energy between **13b** (**MPO-0186**) and mPGES-1 was greater (-194.46 kcal/mol) than that (-168.64 kcal/mol) of **13a** (**MPO-0180**). Therefore, it was rationalized that **13b** (**MPO-0186**) exhibited more potency than **13a** (**MPO-0180**) by establishing stronger hydrogen bonds and hydrophobic interactions with mPGES-1 enzyme. On the other hand, **11a** (**MPO-0063**: scaffold A) don't have a flexible four-methylene unit to afford a compact conformation and exhibited lower MolDock Scrore than that of **13b** (**MPO-0186**). However, the inhibitory activity of **11a** (**MPO-0063**) against m-PGES-1 was found to be equipotent as that of that of **13b** (**MPO-0186**). Based on the detailed analysis of docking results (Supplementary data), **11a** (**MPO-0063**) exhibited additional hydrogen bond interactions with GSH (cofactor) by using the other nitrogen atom of hydrazide moiety and thus could have stronger interaction with GSH than **13b** (**MPO-0186**), capable of strongly inhibiting m-PGES-1 enzyme.

The major side effects of COX-2 inhibitors on the cardiovascular system could be associated with reduced PGI_2 synthesis.[26] Thus, three

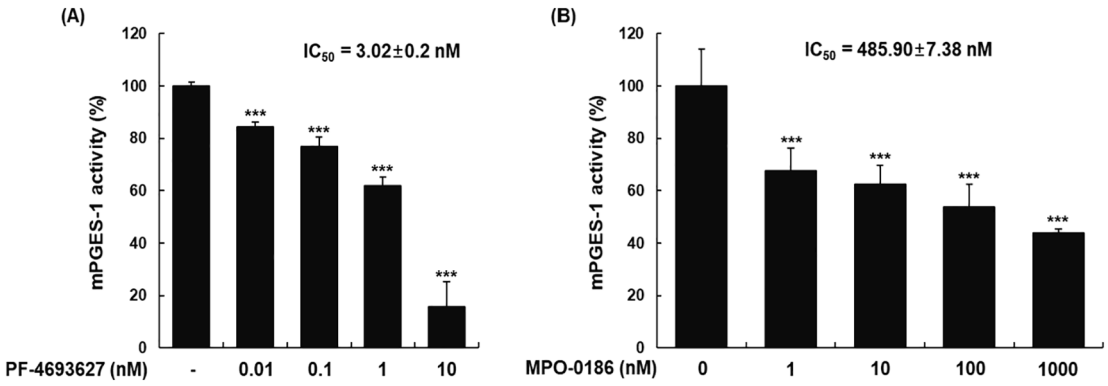

Fig. 4. Effect of **PF-4693627** as a reference inhibitor (A) and compound **13b** (**MPO-0186**) (B) on mPGES-1 activity. Microsomal preparation of IL-1β-stimulated A549 cells were preincubated with indicated concentrations of compounds or vehicle (DMSO) for 15 min on ice. After reactions for 1 min with substrate, PGE_2 production was measured by EIA kits. Remaining activity (% of control) are showed mean ± SDs (n = 3). $^{***}p < 0.001$ vs. the control group; significant differences between groups were determined using ANOVA and Dunnett's post-hoc test.

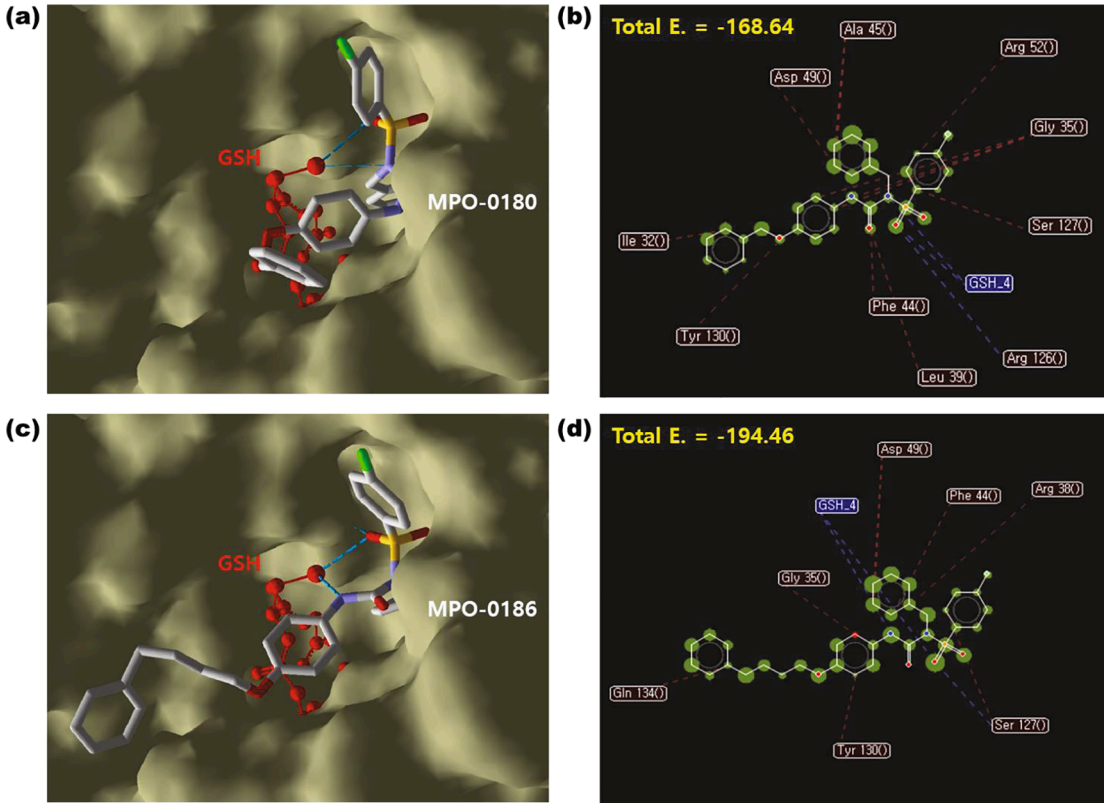

Fig. 5. 3D and 2D docking mode of **MPO-0180** (a-b) and **MPO-0186** (c-d) into the active site of mPGES-1 enzyme. All hydrogen atoms were omitted for the graphic simplicity. Each pose was represented by stick form and colored by element and glutathione as a cofactor was represented by ball-and-stick red colored form. Hydrogen bonds were depicted as blue dashed lines and hydrophobic interactions were depicted as red dashed lines.

scaffold compounds were further screened for the inhibitory effect on the PGI_2 production in A549 cancer cells. As shown in Table 2, compound **11a** (**MPO-0063**) strongly reduced the level of PGI_2 with IC_{50} value of 0.25 μM. However, **12** (**MPO-0112**) and **13b** (**MPO-0186**) could weekly reduce the level of PGI_2 with IC_{50} values of 2.0 and 1.0 μM, respectively. Therefore, **12** (**MPO-0112**) and **13b** (**MPO-0186**) exerted ca. 8- and 4-fold selective inhibitory activities against PGE_2 over PGI_2 production in A549 cancer cells, respectively, when treated with IL-1β.

We also explored the brief drug-like properties of three scaffold compounds through *in vitro* ADME study using the reported standard protocol.[27] Preliminary results of *in vitro* ADME study were listed in Table 2. Firstly, positive and negative predictive values of absolute hERG IC_{50} indicats that from an early drug discovery perspective, compounds with low potency can be progressed on the basis of a low risk of causing a QTc increase: high ($IC_{50} < 1$ μM), intermediate (1 μM < $IC_{50} < 10$ μM), and low ($IC_{50} > 10$ μM).[28] Compounds **11a** (**MPO-0063**) and **13b** (**MPO-0186**) showed low potency against hERG potassium channels with IC_{50} values of 9.6 and > 10 μM, respectively, compared to **12** (**MPO-0112**) with IC_{50} value of 5.2 μM. Next, five CYP450 isozymes were selected to gain a preliminary understanding of the interaction between each compound and the CYP450 isozymes using the standard procedure.[29–30] In this CYP450 assay at 10 μM concentration of each compound, all compounds showed lower inhibition of four CYP450 isozymes ($IC_{50} \geq 10$ μM) except CYP2C19. **13b** (**MPO-0186**) exhibited

high inhibition of only CYP2C19 (8.7% remaining activity of enzyme), which is a liver enzyme that acts on at least 10% of drugs in current clinical use.[31] We also explored the *in vitro* metabolic stability in mouse, rat, dog, and human liver microsomes using a single point metabolic assay.[29,32] Briefly, each compound was incubated at a concentration of 1.0 μM with 1.0 mg/mL protein at 37 °C for 30 min. **11a** (**MPO-0063**) and **12** (**MPO-0112**) exhibited low to intermediate liver metabolic stability depending on the animal (16.3 to 66.6% remaining). However, **13b** (**MPO-0186**) showed good metabolic stability with more than 75% remaining in liver microsomes of all species as shown in Table 2. The *in vitro* stabilities of each 10 μM compound in human and rat plasmas were determined.[29] All compounds were very unstable in rat plasma. However, **12** (**MPO-0112**) and **13b** (**MPO-0186**) exhibited good and moderate human plasma stability (~100 and 45% remaining, respectively, after 30 min). Overall, **13b** (**MPO-0186**) exhibited *in vitro* favorable ADME profiles except CYP2C19 isozyme and plasma stability, indicating that further SAR investigation is needed to improve its ADME profile.

In conclusion, we have shown that *N*-carboxy-phenylsulfonamide (scaffold B) and *N*-amido-phenylsulfonamide (scaffold C) as bioisosteres of *N*-carboxy-phenylsulfonyl hydrazides (scaffold A) could act as a new skeleton for novel mPGES-1 inhibitors. Among them, **13b** (**MPO-0186**) as a new scaffold C derivative exhibited selective inhibitory activity against PGE_2 over PGI_2 production in the A549 cellular assay by inhibiting mPGES-1 enzyme, which was virtually supported by molecular docking study. Furthermore, **13b** (**MPO-0186**) showed the lower binding affinity (IC_{50}: >10 μM) for hERG ion channel, the remarkable liver metabolic stability, and the favorable CYP450 assay profiles except CYP2C19 isozyme. This could be a potential starting point for the development of selective and potent mPGES-1 inhibitor with a novel scaffold.

Declaration of Competing Interest

The authors declare that they have no known competing financial interests or personal relationships that could have appeared to influence the work reported in this paper.

Acknowledgments

This work was supported by the National Research Foundation of Korea (NRF) grant funded by the Korea government (MSIT) (No. 2019R1F1A1059332 and No. 2020R1A5A2019413).

Appendix A. Supplementary data

Supplementary data to this article can be found online at https://doi.org/10.1016/j.bmcl.2021.127992.

References

1 Park JY, Pillinger MH, Abramson SB. *Clin Immunol*. 2006;119:229.
2 Tsuge K, Inazumi T, Shimamoto A, Sugimoto Y. *Int Immunol*. 2019;31:597.
3 Kudo I, Murakami M. *J Biochem Mol Biol*. 2005;38:633.
4 Koeberle A, Werz O. *Curr Med Chem*. 2009;16:4274.
5 Mattila S, Tuominen H, Koivukangas J, Stenbäck F. *Neuropathology*. 2009;29:156.
6 Laine LJ. *Pain Symptom Manag*. 2003;25:S32.
7 Sanghi S, MacLaughlin EJ, Jewell CW, et al. *Cardiovasc Hematol Disord Drug Targets*. 2006;6:85.
8 McGettigan P, Henry D. *JAMA*. 2006;296:1633.
9 Samuelsson B, Morgenstern R, Jakobsson PJ. *Pharmacol Rev*. 2007;59:207.
10 Bergqvist F, Morgenstern R, Jakobsson PJ. *Prostaglandins Other Lipid Mediat*. 2020;147, 106383.
11 Norman BH, Fisher MJ, Schiffler MA, et al. *J Med Chem*. 2018;61:2041.
12 Jin Y, Smith CL, Hu L, et al. *Clin Pharmacol Ther*. 2016;99:274.
13 Sant S, Tandon M, Menon V, et al. *Osteoarthr Cartil*. 2018;26:S351.
14 Lee HH, Moon YH, Shin J-S, et al. *Prostaglandins Other Lipid Mediat*. 2019;144, 106347.
15 Park EB, Kim KJ, Jeong HR, et al. *Bioorg Med Chem Lett*. 2016;26:5193.
16 Kim M, Lee S, Park EB, et al. *Bioorg Med Chem Lett*. 2016;26:94.
17 Park SJ, Han SG, Ahsan HM, et al. *Bioorg Med Chem Lett*. 2012;22:7335.
18 Patani GA, LaVoie EJ. *Chem Rev*. 1996;96:3147.
19 Neuman RG, Korn JH, Lally ET, Wood DD, Kimball ESJ. *Immunoassay*. 1988;9:159.
20 Won JH, Im HT, Kim YH, et al. *Br J Pharmacol*. 2006;148:216.
21 Endo T, Ogushi F, Sone S, et al. *Am J Respir Cell Mol Biol*. 1995;12:358.
22 Arhancet GB, Walker DP, Metz S, et al. *Bioorg Med Chem Lett*. 2013;23:1114.
23 Kim SY, Jung DW, Yoon HB, et al. *Bull. Kor. Chem. Soc*. 2018;39:891.
24 Koeberle A, Siemoneit U, Bühring U, et al. *J Pharmacol Exp Ther*. 2008;326:975.
25 Khurana P, Jachak SM. *RSC Adv*. 2016;6:28343.
26 Day RO, Graham GG. *Aust. Prescr*. 2004;27:142.
27 Li AP. *Drug Discov Today*. 2001;6:357.
28 Pollard CE, Skinner M, Lazic SE, et al. *Toxicol Sci*. 2017;159:94.
29 Choi TA, Furimsky AM, Swezey R, et al. *J Pharm Sci*. 2015;1832:104.
30 Fasinu PS, Gutmann H, Schiller H, Jame A-D, Bouic PJ, Rosenkranz B. *Drug Metab Dispos*. 2013;41:488.
31 Li-Wan-Po A, Girard T, Farndon P, Cooley C, Lithgow J. *Br J Clin Pharmacol*. 2010;69:222.
32 Di L, Kerns EH, Gao N, et al. *J Pharm Sci*. 2004;93:1537.